

Fractional Order PV/T Model Design and Estimation using the Fractional Observer

Amer Aziz¹, Muwahida Liaquat¹, Aamer Iqbal Bhatti² and Lahoucine Ouhsaine³

¹National University of Sciences and Technology, Pakistan

²Capital University of Science and Technology, Pakistan

³Université de Lorraine Nancy, France

Keywords: Fractional-order System, PV/T Hybrid System, Observation, Fractional-HOSMO, Estimation, Disturbance, Pseudo State.

Abstract: In the last decade, the demand for renewable energy sources has been increased due to factors which include the rising fuel price and pollution, and consequently research on solar energy sources has been increased to improve their efficiency. Photovoltaic Thermal (PV/T) system provides electrical power and heat simultaneously, which is the promising technology. This research paper illustrates the simulation of the comprehensive thermal-based mathematical model of the PV/T system with the joint estimation of the system states: the temperature at each node, and disturbance using Fractional-High Order Sliding Mode Observer (HOSMO). A fractional-order differential equation describes the PV/T system because of its characterization in heterogeneous media and its multilayers structure. Fractional-HOSMO is a robust observer that can be used further for the reduced-sensor control of PVT, which can be comparatively cheap. The parameter values are derived from the thermal configuration of the layers and the properties of constituents.

1 INTRODUCTION

The photovoltaics (PV) system is affected by external climatic conditions, so its electrical efficiency decreases rapidly as its temperature increases. In recent years, researchers have studied PV/T, which combines both PV solar cells and thermal collectors to enhance the overall efficiency and performance (Lobera, 2013; Cui Young, Abd El-Samie and Alayi, 2020). The impact and importance of heat transfer fluid like water, air, nanofluids, and the other fluid types have been described on the characterization and performance of the PV/T system (Esfe, Eisapour, Salari and Alayi, 2020; Jiang Q, 2018). A water-based PV/T system is commonly used in domestic because it is quite simple and economical as compared to other types. It shows improved performance and enhanced efficiency of the thermal PV/T from the indoor and outdoor experiments (Al-Waeli, 2018). A thermal-based model for the PV module, integrated with a solar air collector, is presented. The PV module temperature can be minimized and controlled from changing the mass flow rate of air to optimize the performance of the module (Joshi, 2009). The thermal and electrical-based model of PVT is designed to study the rational behaviour of

thermal and electrical parameters such as PV temperature, fluid outlet temperature, and open-circuit voltage in (Sarhaddi, 2010). A thermal model of building and heat transfer in heterogeneous media has designed using a fractional-order approach. Fractional derivative order is an indicator of the building's heat capacity (Skruch, 2013). In (Sierociuk, 2013), general equations for heat process in heterogeneous media is suggested by considering dispersed heat flux in the air around the beam. A fractional-order partial differential equation is derived for the sub or hyper diffusion process in that particular media.

Fractional differentiation operator is the generalized form of the simple integer differentiation operator. It is crucial to model real-world phenomena because of its hereditary properties and applications, and many basic concepts of control field like observability, controllability concepts and stability condition has extended to general FOS (Monje, 2010; Sabatier, 2012; Birs, Yıldız, Giusti and Acay, 2020). A generalized thermal-based PV/T system model is discussed in (Ouhsaine et al., 2017). The performance of the fractional observer is explained for the proposed fractional-order systems for pseudo-state estimation (Belkhatir, 2017). Many authors suggest

the integer-based high order sliding mode observer using Levant differentiator under unknown input (Levant, 2007; Chu and Feng, 2020).

This paper presents the fractional-order thermal-based model of the PVT system in state-space representation. Irradiation factor and PV cell parameters, which are very critical to the PV/T, are also taken into account in the proposed system. System states and disturbances are estimated by using fractional order high order sliding mode observer from the output temperature state of the PV/T system under some disturbance. The impact of the differentiator gain of the observer is explained in the estimation of states and disturbance.

The structure of this research paper as follows: Section 2 describes the main problem statement and a thermal-based model of the PV/T model by fractional-order equations in state-space representation. Fractional HOSMO is presented for the system under disturbance in section 3. Simulation is performed to illustrate its performance under disturbance for the pseudo-states and disturbance estimation of the given system, and the effect of the differentiator gain on estimation error in section 4. The research paper is concluded and delivers the outlines for future work in section 5.

2 PROBLEM STATEMENT

External Temperature, Irradiation, and fluid temperature are the inputs which have been applied to the PV/T system in Figure 1.

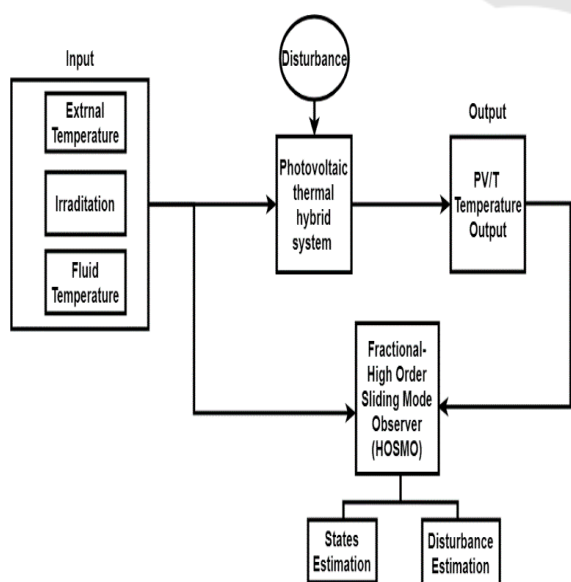


Figure 1: Disturbance & States estimation of the system.

The main objective is to estimate all the temperature states of PV/T model design described by the fractional-order differential equations because of its characterization in heterogeneous media and its multilayers structure.

Fractional- HOSMO is used to estimate all the node temperatures of each layer and disturbance using the PV cell temperature as output. Fractional HOSMO uses differentiators to converge the estimated temperature states on the actual temperature states.

3 PVT MATHEMATICAL MODELLING

3.1 System Description

PV/T converts sunlight into electricity from the solar cell, and it captures the residual heat energy and eliminates it from the PV module using the solar thermal collector. Figure 2 elaborates on the essential heat transfer principle and specific arrangements of its components in the 2D scheme.

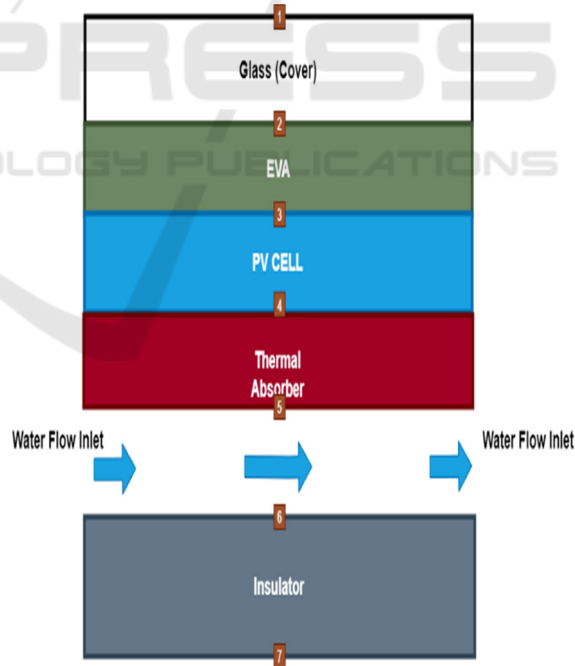


Figure 2: PV/T multilayer structure.

In the first layer, there is a glass cover that provides more extended durability to the solar cells and higher design flexibility compared to other encapsulating technologies. Then, the second layer is made of Ethylene-vinyl acetate (EVA), which is an

electrical insulator. The third layer is the PV cell, which is the most crucial component to generate electricity from solar irradiation. In the fourth layer, a copper absorber is employed to absorb the extra heat directly from PV cells. After these layers, a heat exchanger flows under fixed small channels to extract the excessive heat from the system. The use of base heat transfer fluid (HTF) is essential to ensure better cooling for the PV panel and heat gain for the thermal system's output. Then this thermal energy can be utilized for domestic use or heating purposes. In this particular model, the heat transfer fluid is water. In the last layer, there is a thermal insulator, which prevents the heat flows through the sink.

3.2 Mathematical Modelling

Let assume the HTF (water) temperature is uniform. Then, the following equation proposes the dynamic behaviour issued from the thermal balances in each layer.

Following equation describes the fractional based heat diffusion (Ouhaine et al., 2017):

$$H(t, \lambda) = \kappa \frac{\partial^\alpha}{\partial t^\alpha} T(t, \lambda) \quad (1)$$

$$\rho_i c_i e_i \frac{d^\alpha T_i}{dt} = Q_i^{in} - Q_i^{out} \quad (2)$$

Where i is the index number for each layer, and ρ, c, e correspond to density, heat capacity, and thickness of manufacturing materials in each layer, respectively

$$\rho_i c_i e_i \frac{d^\alpha T_i}{dt} = U_{i-1}(T_{i-1} - T_i) - U_i(T_i - T_{i+1}) \quad (3)$$

Fractional state-space representation:

$$\begin{aligned} D_t^\alpha x(t) &= Ax(t) + Bu(t) \\ y(t) &= Cx(t) \end{aligned} \quad (4)$$

Where A is the state matrix, B is the input matrix, C is the input matrix of the system.

System matrix (A) is

$$A = \begin{bmatrix} -\left(\frac{(h_{ext}) + U_1}{(\rho c e)_1}\right) & \frac{U_1}{(\rho c e)_1} & 0 & 0 & 0 & 0 & 0 \\ \frac{U_1}{(\rho c e)_2} & -\frac{(U_1 + U_2)}{(\rho c e)_2} & \frac{U_2}{(\rho c e)_2} & 0 & 0 & 0 & 0 \\ 0 & \frac{U_2}{(\rho c e)_3} & -\frac{(U_2 + U_3)}{(\rho c e)_3} & \frac{U_3}{(\rho c e)_3} & 0 & 0 & 0 \\ 0 & 0 & \frac{U_3}{(\rho c e)_4} & -\frac{(U_3 + U_4)}{(\rho c e)_4} & \frac{U_4}{(\rho c e)_4} & 0 & 0 \\ 0 & 0 & 0 & \frac{U_4 t_c}{(\rho c e)_5} & -\frac{(U_4 + U_5)}{(\rho c e)_5} & \frac{U_5}{(\rho c e)_5} & 0 \\ 0 & 0 & 0 & 0 & \frac{U_5}{(\rho c e)_6} & -\frac{(U_5 + U_6)}{(\rho c e)_6} & \frac{U_6}{(\rho c e)_6} \\ 0 & 0 & 0 & 0 & 0 & \frac{U_6}{(\rho c e)_7} & -\frac{(U_6 + U_7)}{(\rho c e)_7} \end{bmatrix}$$

Input matrix (B) is

$$B = \begin{bmatrix} \frac{h_{ext}}{\rho_1 c_1 e_1} & 0 & 0 \\ 0 & \frac{1 - \eta_{pv}}{\rho_2 c_2 e_2} e_2 & 0 \\ 0 & 0 & 0 \\ 0 & 0 & \frac{\dot{m} c_f}{\rho_4 c_4 e_4} \\ 0 & 0 & 0 \\ 0 & 0 & 0 \\ 0 & 0 & 0 \end{bmatrix}$$

Where $x(t) = [T_1, T_2, T_3, \dots, T_7]$ is the state vector of temperature at each node, and $u(t) = [Text, G, T_f]$ is the input vector, here $G, Text$ & T_f are irradianations, external temperature, and fluid temperatures respectively.

4 FRACTIONAL HIGH ORDER SLIDING MODE OBSERVER

Many sensors are required for the measurement of states, so they are costly and complicated. System state measurements may be too noisy due to the presence of disturbance. Therefore, to solve this problem, system states are estimated by the help of Fractional HOSMO. The advantage of this observer is that it also estimates the disturbance added in the system if it is bounded.

Following assumptions should be satisfied by the system (Belkhatir, 2017):

- Assumption 1: The system should be completely observable
- Assumption 2: The relative degree of the system concerning unknown input should be n . It shows that the system is strongly observable.
- Assumption 3: The unknown input and its derivative should be bounded a function of Lebesgue measurable.

The following equations give fractional HOSMO:

$$D_t^\alpha z(t) = Az(t) + Bu(t) + L(y - Cz(t)) \quad (5)$$

$$\begin{cases} D_t^\alpha v_1 = w_1 = v_2 - \lambda_{n+1} M^{\frac{1}{n}} |v_1 - y + Cz|^{\frac{n}{n+1}} \text{sign}(v_1 - y + Cz) \\ D_t^\alpha v_2 = w_2 = v_3 - \lambda_n M^{\frac{1}{n}} |v_2 - w_1|^{\frac{n-1}{n}} \text{sign}(v_2 - w_1) \\ \vdots \\ D_t^\alpha v_{n+1} = -\lambda_1 M \text{sign}(v_{n+1} - w_n) \end{cases} \quad (6)$$

$$\hat{x}(t) = z(t) + Kv(t) \quad (7)$$

$$\hat{\xi}(t) = 1/d [v_{n+1} - (a_1 v_1 + \dots + a_n v_n)] \quad (8)$$

Where $z \in \mathbb{R}^n$ and $L \in \mathbb{R}$ is the vector and gain of Luenberger observer (5) respectively, $v \in \mathbb{R}^{n+1}$ and M is the vector and gain of differentiator (6) respectively where the sliding surface is defined, constant $d = C(A - LC)^{n-1}$, \hat{x} is pseudo-state estimation vector and K is a correction gain which is inverse of observability matrix in (7), $a_i \in \mathbb{R}$ are coefficients of $K^{-1}(A - LC)K$ in the estimation of disturbance $\zeta(t)$.

5 SIMULATION

Table 1: The values of important parameters.

Serial #	Material	Thermal conductivity K (w/mk)	Thickness Of layers (mm)	Densities (kg/m ³)	Heat Capacity (J/kg k)
1	Glass	0.98	2	2500	820
2	PV Cell	134	0.3	2329	713
3	EVA	0.23	0.5	957	760
4	Thermal absorber	400	0.5	8700	385
5	Fluid (water)	0.5918	1	997	4185.5
6	Glass fiber Slab (insulator)	0.035	10	25	1000

The simulation illustrates the performance of the observer for the given PV/T system. There are two cases:

- I. Disturbance free
- II. Disturbed system

Now after putting the values of parameters as given in table 1, system matrices are as follow:

$$A = \begin{bmatrix} -1.19 & 0.180 & 0 & 0 & 0 & 0 & 0 \\ 0.41 & -0.61 & 0.24 & 0 & 0 & 0 & 0 \\ 0 & 0.79 & -1000.5 & 1001 & 0 & 0 & 0 \\ 0 & 0 & 202 & -298 & 96 & 0 & 0 \\ 0 & 0 & 0 & 56.1 & -56.7 & 0.14 & 0 \\ 0 & 0 & 0 & 0 & 2.36 & -2.30 & 0.01 \\ 0 & 0 & 0 & 0 & 0 & 1 & -20.70 \end{bmatrix}$$

The parameter values are taken from the manual of the apparatus (PVT system) in the laboratory of National University of Sciences and Technology Islamabad, Pakistan.

The output matrix will be

$$C = [0 \ 0 \ 0 \ 0 \ 0 \ 0 \ 1]$$

The following system is observable. The system is at rest and taking initial condition zero. Inputs is [30,900,18]. The different values of input can be taken according to the model.

5.1 Case 1: Disturbance Free

Differentiator gain is $M=5$, and the gain of the linear observer part is $L = [500 \ 100 \ 15 \ 20 \ 5 \ 10 \ 5]^T$

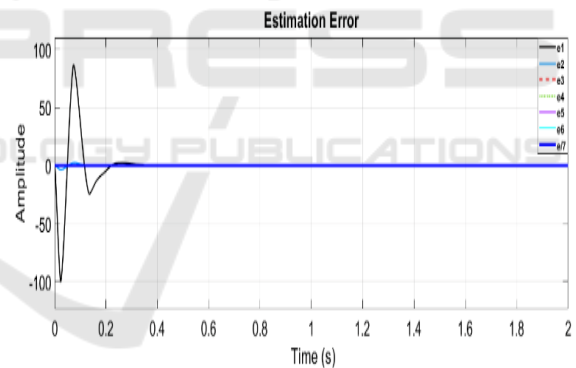


Figure 3: States estimation error without disturbance.

Figure 3 shows that, in the absence of unknown input or disturbance, HOSMO will simultaneously ignore modeling ambiguity and easily estimate the system states.

5.2 Case 2: Under Disturbance

In this case, the system has perturbed by incorporating the disturbance in the first state of the system. The observer should estimate it accurately so that some suitable controller can eliminate its effect using this disturbance estimation. The disturbance added in the system is $\zeta(t) = 10\sin(2\pi t)$. Differentiator gain is $M=25$.

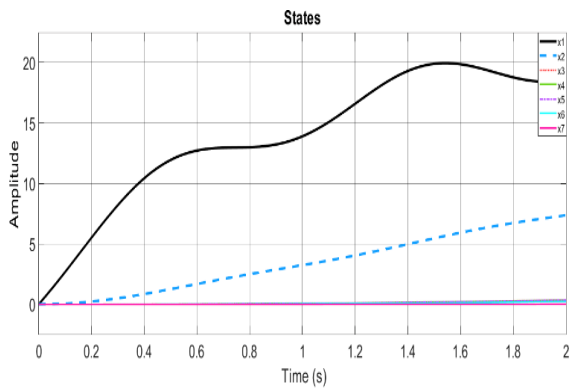


Figure 4: System states under the disturbance.

Figure 4 shows the effect of the disturbance in which systems states have been disturbed. System state showing the nonlinear behaviour due to nonlinear disturbance.

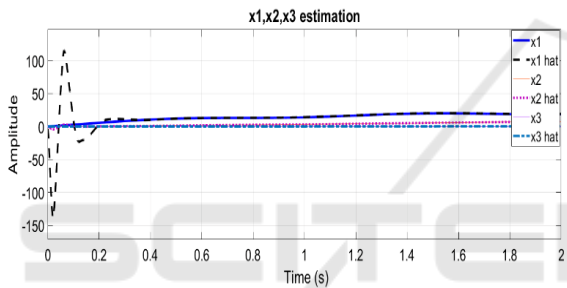


Figure 5: States x_1, x_2, x_3 and their estimated states.

Figure 5 shows that the estimated states of (T1-T3) converging on the system states at 0.25 second.

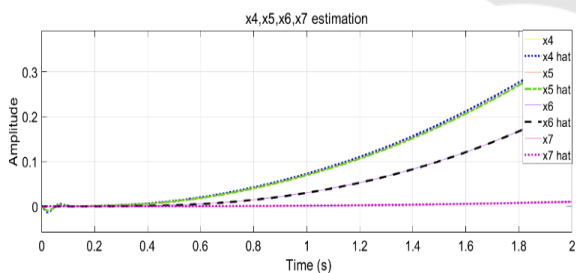


Figure 6: States x_4, x_5, x_6, x_7 and their estimated states.

Figure 6 shows that the estimated states of (T4-T7) converging on the system states at 0.15 second.

It is shown that observer is still estimating the status smoothly under the disturbance because all the estimated states of the observer are converging to the systems states smoothly within 0.25 sec in Figures 5 and 6.

5.2.1 Estimation Error for Observer

The estimation error is the measure of the performance of the given observer.

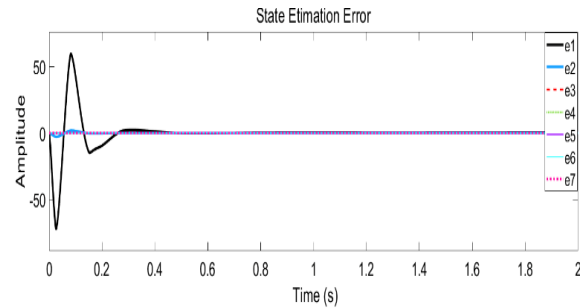


Figure 7: The estimation error for all the states.

Figure 7 shows that the estimation error for all states is zero when all the estimated states converge to the system states within 0.25 second.

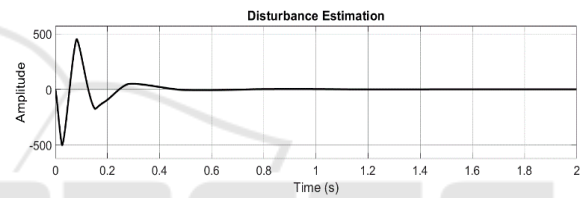


Figure 8: The estimation error for disturbance.

Figure 8 shows that the estimation error for disturbance is zero when the estimation of disturbance is converging to the actual disturbance within 0.3 second.

It is shown in figures 7 and 8 that states and disturbance estimation error is high in the start, but it becomes zero at 0.25 sec when estimated states converge on system states. Therefore, these graphs are evidence of the excellent performance of the given observer.

5.2.2 Effect of the Gain M

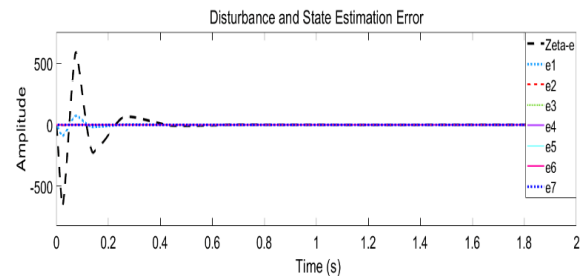


Figure 9: State-estimation errors for $M=50$.

It illustrates the effect of the differentiator gain M on the convergence and amplitude of error. There exists a compromise between convergence and overshoot of estimation error.

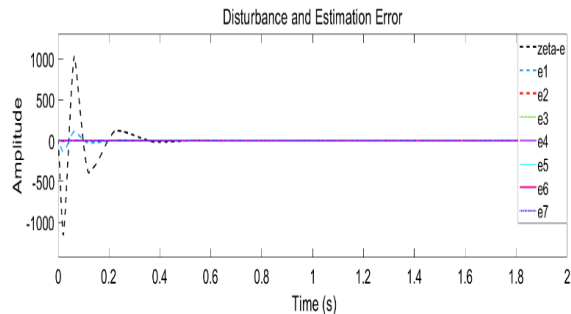


Figure 10: State-estimation errors for $M=200$.

The overshoot of estimation error is increasing from 600 to 1000 as gain is increasing from 50 to 200. While the convergence in the second scenario will be better than in the first scenario

Figures 9 and 10 elaborate that there exists a trade-off between estimation convergence and the overshoot of estimation error because, when M gain is increased, the overshoot of the estimation error will also increase.

6 CONCLUSIONS

This paper presents the thermal-based modelling of the multilayer structure PVT system by a fractional-order derivative equation and then its state-space representation. Fractional-HOSMO is implemented to estimate the disturbance and system states under disturbance. Simulation is performed to test the performance of the given observer for both cases: disturbance-free and disturbed systems. It describes the effect of the gain on the performance of the observer. It emphasizes on the hardware implementation of this system and extends it to the multiple inputs and multiple outputs system for future work. It will be interesting to make further suggestions for improvements in the system.

REFERENCES

Lobera, D. T., & Valkealahti, S. (2013). Dynamic thermal model of solar PV systems under varying climatic conditions. *Solar energy*, 93, 183-194.
 Cui, Y., Yao, H., Zhang, J., Xian, K., Zhang, T., Hong, L., ... & Hou, J. (2020). Single - junction organic

photovoltaic cells with approaching 18% efficiency. *Advanced Materials*, 32(19), 1908205.
 Abd El-Samie, M. M., Ju, X., Zhang, Z., Adam, S. A., Pan, X., & Xu, C. (2020). Three-dimensional numerical investigation of a hybrid low concentrated photovoltaic/thermal system. *Energy*, 190, 116436.
 Alayi, R., Kasaeian, A., & Atabi, F. (2020). Optical modeling and optimization of parabolic trough concentration photovoltaic/thermal system. *Environmental Progress & Sustainable Energy*, 39(2), e13303.
 Esfe, M. H., Kamyab, M. H., & Valadkhani, M. (2020). Application of nanofluids and fluids in photovoltaic thermal system: An updated review. *Solar Energy*, 199, 796-818.
 Eisapour, M., Eisapour, A. H., Hosseini, M. J., & Talebizadehsardari, P. (2020). Exergy and energy analysis of wavy tubes photovoltaic-thermal systems using microencapsulated PCM nano-slurry coolant fluid. *Applied Energy*, 266, 114849.
 Salari, A., Kazemian, A., Ma, T., Hakkaki-Fard, A., & Peng, J. (2020). Nanofluid based photovoltaic thermal systems integrated with phase change materials: numerical simulation and thermodynamic analysis. *Energy Conversion and Management*, 205, 112384.
 Alayi, R., Kasaeian, A., & Atabi, F. (2020). Optical modeling and optimization of parabolic trough concentration photovoltaic/thermal system. *Environmental Progress & Sustainable Energy*, 39(2), e13303.
 Yu, B., Jiang, Q., He, W., Liu, S., Zhou, F., Ji, J., ... & Chen, H. (2018). Performance study on a novel hybrid solar gradient utilization system for combined photocatalytic oxidation technology and photovoltaic/thermal technology. *Applied Energy*, 215, 699-716.
 Al-Waeli, A. H., Chaichan, M. T., Kazem, H. A., Sopian, K., Ibrahim, A., Mat, S., & Ruslan, M. H. (2018). Comparison study of indoor/outdoor experiments of a photovoltaic thermal PV/T system containing SiC nanofluid as a coolant. *Energy*, 151, 33-44.
 Joshi, A. S., Tiwari, A., Tiwari, G. N., Dincer, I., & Reddy, B. V. (2009). Performance evaluation of a hybrid photovoltaic thermal (PV/T)(glass-to-glass) system. *International Journal of Thermal Sciences*, 48(1), 154-164.
 Sarhaddi, F., Farahat, S., Ajam, H., Behzadmehr, A. M. I. N., & Adeli, M. M. (2010). An improved thermal and electrical model for a solar photovoltaic thermal (PV/T) air collector. *Applied energy*, 87(7), 2328-2339.
 Skruch, P. (2013). A general fractional-order thermal model for buildings and its properties. In *Advances in the Theory and Applications of Non-integer Order Systems* (pp. 213-220). Springer, Heidelberg.
 Sierociuk, D., Dzieliński, A., Sarwas, G., Petras, I., Podlubny, I., & Skovranek, T. (2013). Modelling heat transfer in heterogeneous media using fractional calculus. *Philosophical Transactions of the Royal Society A: Mathematical, Physical and Engineering Sciences*, 371(1990), 20120146.

- Monje, C. A., Chen, Y., Vinagre, B. M., Xue, D., & Feliu-Batlle, V. (2010). *Fractional-order systems and controls: fundamentals and applications*. Springer Science & Business Media.
- Sabatier, J., Farges, C., Merveillaut, M., & Feneteau, L. (2012). On observability and pseudo state estimation of fractional order systems. *European journal of control*, 18(3), 260-271.
- Birs, I., Nascu, I., Ionescu, C., & Muresan, C. (2020). Event-based fractional order control. *Journal of Advanced Research*.
- Yıldız, T. A., Jajarmi, A., Yıldız, B., & Baleanu, D. (2020). New aspects of time fractional optimal control problems within operators with nonsingular kernel. *Discrete & Continuous Dynamical Systems-S*, 13(3), 407.
- Giusti, A. (2020). General fractional calculus and Prabhakar's theory. *Communications in Nonlinear Science and Numerical Simulation*, 83, 105114.
- Acay, B., Bas, E., & Abdeljawad, T. (2020). Non-local fractional calculus from different viewpoint generated by truncated M-derivative. *Journal of Computational and Applied Mathematics*, 366, 112410.
- Ouhsaine, L., Boukal, Y., El Ganaoui, M., Darouach, M., Zasadzinski, M., Mimet, A., & Radhy, N. E. (2017). A General fractional-order heat transfer model for Photovoltaic/Thermal hybrid systems and its observer design. *Energy Procedia*, 139, 49-54.
- Belkhatir, Z., & Laleg-Kirati, T. M. (2017). High-order sliding mode observer for fractional commensurate linear systems with unknown input. *Automatica*, 82, 209-217.
- Levant, A. (2003). Higher-order sliding modes, differentiation and output-feedback control. *International journal of Control*, 76(9-10), 924-941.
- Fridman, L., Levant, A., & Davila, J. (2007). Observation of linear systems with unknown inputs via high-order sliding-modes. *International Journal of systems science*, 38(10), 773-791.
- Ferreira de Loza, A., Fridman, L., Aguilar, L. T., & Iriarte, R. (2019). High - order sliding - mode observer-based input - output linearization. *International Journal of Robust and Nonlinear Control*, 29(10), 3183-3199.
- Yin, X., Wang, B., Liu, L., & Wang, Y. (2019). Disturbance observer-based gain adaptation high-order sliding mode control of hypersonic vehicles. *Aerospace Science and Technology*, 89, 19-30.
- Chu, Z., Meng, F., Zhu, D., & Luo, C. (2020). Fault reconstruction using a terminal sliding mode observer for a class of second-order MIMO uncertain nonlinear systems. *ISA transactions*, 97, 67-75.
- Feng, Z., Liang, W., Ling, J., Xiao, X., Tan, K. K., & Lee, T. H. (2020). Integral terminal sliding-mode-based adaptive integral backstepping control for precision motion of a piezoelectric ultrasonic motor. *Mechanical Systems and Signal Processing*, 144, 106856.